MODELLING APPROACH FOR BRUSHLESS DC MOTOR DIAGNOSTICS

YURY NIKITIN[1], SERGEI TREFILOV[1]

[1]Department of Mechatronic Systems, Kalashnikov Izhevsk State Technical University, Izhevsk, Udmurtia

DOI: 10.17973/MMSJ.2025_12_2025106

nikitin@istu.ru

Annotation. A brushless DC (BLDC) motors diagnostics system based on the model approach in the state space is developed. A digital twin representing a model of BLDC motor and working in parallel with a real BLDC motor is designed. The BLDC motor are analyses using electric current and angular velocity sensors signals and the output signals of the digital twin. Based on the magnitude of the residual, the presence of defects in the real BLDC motor is determined. If the defect value is insignificant, then appropriate maintenance actions are recommended. In case when the defect value is significant, it is necessary to perform emergency termination of the engine operation.

KEYWORDS

diagnostics, model, brushless DC motor, residual, defects

1 INTRODUCTION

Nowadays, electric motors have been widely used in industry and transport due to their simple design, low cost. To improve reliability, their diagnostics is required. There are various methods of diagnostics of electric motors described in [Chen 2021, Zhou 2020]. Brushless direct current (BLDC) motors are mostly preferred for dynamic applications such as automotive industries, pumping industries, and rolling industries. It is predicted that by 2030, BLDC motors will become mainstream of power transmission in industries replacing traditional induction motors. Though the BLDC motors are gaining interest in industrial and commercial applications, the future of BLDC motors faces indispensable concerns and open research challenges. Considering the case of reliability and durability, the BLDC motor fails to yield improved fault tolerance capability, reduced electromagnetic interference, reduced acoustic noise, reduced flux ripple, and reduced torque ripple. To address these issues, closed-loop vector control is a promising methodology for BLDC motors. In the literature survey of the past five years, limited surveys were conducted on BLDC motor controllers and designing. Moreover, vital problems such as comparison between existing vector control schemes, fault tolerance control improvement, reduction in electromagnetic interference in BLDC motor controller, and other issues are not addressed. This encourages the author in conducting this survey of addressing the critical challenges of BLDC motors. Furthermore, comprehensive study on various advanced controls of BLDC motors such as fault tolerance control, Electromagnetic interference reduction, field orientation control (FOC), direct torque control (DTC), current shaping, input voltage control, intelligent control, drive-inverter topology, and its principle of operation in reducing torque ripples are discussed in detail. This paper also discusses BLDC motor history, types of BLDC motor, BLDC motor structure, Mathematical modeling of BLDC and BLDC motor standards for various applications [Mohanraj 2022].
The study [Xue 2018] deals with the problem of fault detection (FD) for linear discrete time-varying (LDTV) systems by combining the parity space-based method with the stationary wavelet transform (SWT). For the purpose of achieving good FD performance and simultaneously reducing the online computational burden resulted by high parity space order, SWT on residual signal is the first step in this study. This allows the formulation of residual generation as the selection of wavelet basis for SWT and the design of time-varying parity space vectors in a framework of multiscale optimisation. A recursive algorithm is developed for the computation of optimal parity space vectors and based on this; a bank of residual signals can be obtained. Moreover, a weighted multiscale residual evaluation strategy is presented to detect the occurrence of a fault. The major contribution of the study lies in the development of a recursive design of SWT aided parity space vectors, which delivers an improvement of FD performance for a lower parity space order and an easy online implementation. A numerical example is demonstrated to illustrate the effectiveness of the proposed method. There are 2 main approaches: data-based [Cheng 2022, Cheng 2023, Luo 2020], and model-based [Nikitin 2020]. Model-based diagnostic methods are well studied and there are a large number of publications on this subject, for example, [Cioboata 2020, Bozek 2021, Patlolla 2021, Krenicky 2022, Nikitin 2022].
The increased complexity and intelligence of automation systems require the development of intelligent fault diagnosis (IFD) methodologies. Intelligent methods for diagnosing faults are described in the paper [Chen 2022]. By relying on the concept of a suspected space, this study develops explainable data-driven IFD approaches for nonlinear dynamic systems. An important result obtained is a unified form of kernel representations, applicable to both unsupervised and supervised learning. This article´s contribution lies in proposing and formalizing the fundamental concepts for explainable intelligent learning methods, contributing to system modeling and data-driven IFD designs for nonlinear dynamic systems.
A special case of the model-based approach is the observer-based method [Yang 2015]. The paper [Zhou 2018] studies the fault detection problem in ship propulsion systems based on randomized algorithms. The nominal propulsion system model, model with uncertainties and model with additive and multiplicative faults are first addressed in the form of normalized left coprime factorization, respectively. The-gap metric is then introduced to measure how far the system deviates from the nominal operation. To reduce the conservatism in the norm-based threshold, a threshold setting law and the estimation of fault detection rate are formulated on the probabilistic assumption of uncertain and faulty parameters. The simulation results on the ship propulsion system show that the randomized technique is an efficient solution to deal with the fault detection issues [Halko 2014, Mascenik 2022].
The article [Zhang 2024] proposes a new deadbeat predictive current control (DPCC) method based on a sliding-mode observer (SMO), which is applied in the field of permanent magnet motor control. A novel DPCC control method based on SMO is proposed according to the inherent issues of DPCC, which can effectively suppress internal parameter mismatch disturbances and external disturbances in the current loop. The mathematical model and derivation process of the proposed method are introduced. A simulation model is built, and the effectiveness of the proposed method is verified. An experimental platform is built, and the superiority of the proposed method is verified based on comparative experiments. Experimental results show that the proposed algorithm has strong robustness to the motor parameter mismatch. Compared with extended state observer and adaptive observer, the proposed algorithm has faster response speed and higher steady-state accuracy.

Another variant is the digital twin approach. The work [Ding 2019] is an attempt to establish a probabilistic framework for the assessment and design of observer-based fault detection systems. The fundament of our study is randomized algorithms methods which are successfully applied to deal with uncertainty issues in robust control. For our purpose, probabilistic parameter models for faults and model uncertainties are first introduced. The main focus of our work is on the development of randomized algorithms for the assessment of false alarm rate, fault detection rate and mean time to detection as well as for the design of observer-based fault detection systems. To illustrate the potential applications of the proposed algorithms and methods, benchmark study on a real three-tank system is included.

An open-loop BLDC motor output with hardware support and a three-segment method on closed-loop BLDC motor were both examined in the study [Demcak 2024]. The research provides a brushless DC motor model that considers the motor's commutation behavior. To make sure that the drive system for BLDC motors works properly, it is important to know the exact torque value, which is based on the back-EMF. The BLDC motor is simulated in MATLAB/Simulink after a basic mathematical model is developed. In open-loop circuits, the intensity may be adjusted by varying the pulse width (or duty), and the motor speed can be increased or decreased by altering the input voltage. Pulse widths and speeds are measured and compared to real-world hardware in this study. This paper presents a comparison of the outcomes of the BLDC motors based on the examination of time responses.

The purpose of this work is to study the possibility of using a digital twin of a BLDC motor, which can be used for diagnostics. A digital twin works in parallel with the real engine. The output signals from angular velocity and electric current sensors of the motor and the digital twin are analysed. Then the magnitude of the residual is used to determine the presence of BLDC motor defects.

2 DEVELOPMENT OF BRUSHLESS DC DEFECT MOTOR MATHEMATICAL MODEL IN THE STATE SPACE

The development of BLDC motor model of an initially starts with differential equations that describe the electrical and mechanical parts of the motor. The motor model is then written in discrete vector matrix form in the state space.

The motor is always affected by perturbations caused by external factors such as drag torque, measurement errors, parameter errors and additive defects, the BLDC motor model in discrete vector matrix form in state space is extended as follows:

$$\mathbf{x}_{k+1} = \mathbf{A}\mathbf{x}_k + \mathbf{B}\mathbf{u}_k + \mathbf{E}_d\mathbf{D}_k + \boldsymbol{\xi}_k + \mathbf{E}_f\,\mathbf{f}_k, \quad (1)$$

$$\boldsymbol{y}_k = \mathbf{C}\mathbf{x}_k + \mathbf{F}_d\mathbf{D}_k + \boldsymbol{v}_k + \mathbf{F}_f\,\mathbf{f}_k, \quad (2)$$

where $\mathbf{x}_k$ is state vector, $\mathbf{y}_k$ is measurement vector, k is discrete time samples, **A** is state matrix, **B** is control matrix, **C** is measurement matrix, $\mathbf{u}_k$ is control vector; $\mathbf{E}_d$ and $\mathbf{F}_d$ are noise matrices of corresponding dimensions; $\mathbf{D}_k$ is deterministic unknown input vector; $\boldsymbol{\xi}_k$ is random variable depending on the system operation, considered to be normally distributed; $\mathbf{v}_k$ is random variable of noise measurement, considered to be normally distributed; $\mathbf{f}_k$ is additive vector of defects, independent of **u** and $\mathbf{x}_k$; $\mathbf{E}_f$ and $\mathbf{F}_f$ are defect distribution matrices of corresponding dimensions.

The matrices $\mathbf{E}_f$ and $\mathbf{F}_f$, may represent different defects in the engine. In the presence of a defect vector $\mathbf{f}_k$, which is a function of the motor state and input variables, the above representation can also describe multiplicative defects and the stability of motor control may be compromised.

The discrete BLDC motor model is represented as a vector-matrix equation in the state space.

$$\begin{bmatrix} I_d(k+1) \\ I_q(k+1) \\ \omega(k+1) \\ \theta(k+1) \end{bmatrix} = \begin{bmatrix} 1 - T\frac{R_s}{L_d} & Tp\omega(k) & 0 & 0 \\ -Tp\omega(k) & 1 - T\frac{R_s}{L_q} & T\frac{-p\psi}{L_q} & 0 \\ 0 & \frac{p\psi}{J} & 1 - T\frac{F}{J} - T\frac{M(k)-M_L}{J\hat{\omega}(k)} & 0 \\ 0 & 0 & T & 1 \end{bmatrix} \begin{bmatrix} I_d(k) \\ I_q(k) \\ \omega(k) \\ \theta(k) \end{bmatrix} + \begin{bmatrix} \frac{T}{L_d} & 0 \\ 0 & \frac{T}{L_q} \\ 0 & 0 \\ 0 & 0 \end{bmatrix} \begin{bmatrix} U_d(k) \\ U_q(k) \end{bmatrix}, \quad (3)$$

where $I_d(k+1)$ is projection of the stator current onto the ***d*** axis at a time $k+1$;

$I_q(k+1)$ is projection of the stator current onto the ***q*** axis at a time $k+1$;

where $I_d(k)$ is projection of the stator current onto the ***d*** axis at a time k;

$I_q(k)$ is projection of the stator current onto the ***q*** axis at a time k;

$\omega(k+1)$ is the BLDC motor angular velocity at time $k+1$;

$\omega(k)$ is the BLDC motor angular velocity at time k;

$\theta(k+1)$ is the BLDC motor angular displacement at time $k+1$;

$\theta(k)$ is the BLDC motor angular displacement at time k;

T is the sampling interval, the time between $k+1$ and ***k*** counts;

R_s is the active resistance of the BLDC motor stator winding;

L_q, L_d are the inductors of the BLDC motor stator along the ***q*** and ***d*** axes;

p is the number of pairs of BLDC motor poles;

ψ is the magnetic flux induced by permanent magnets in the stator winding;

F is the coefficient of BLDC motor viscous friction force;

J is the moment of inertia;

M is the BLDC motor electromagnetic moment;

U_q, U_d are the projections of the BLDC motor stator voltage on the ***q*** and ***d*** axes.

The required torque is calculated using the formula (4):

$$\hat{M}(k) - M_L = \varepsilon(k)J = \frac{\omega(k+1)-\hat{\omega}(k)}{T}J. \quad (4)$$

The BLDC motor angular velocity is calculated using the formula (5):

$$\hat{\omega}(k) = \frac{\hat{\theta}(k)-\hat{\theta}(k-1)}{T} \quad (5)$$

where $\omega(k+1)$ is the angular velocity at at a time $k+1$ of the trajectory;

$\hat{\omega}(k)$ is the measured angular velocity (or velocity estimate);

$\hat{\theta}(k)$, $\hat{\theta}(k-1)$ are the measured angular positions of the rotor at times $\mathbf{T}(k)$ and $\mathbf{T}(k-1)$, respectively;

$\varepsilon(k)$ is the calculated acceleration to reach the trajectory velocity $\omega(k+1)$ at time $(k+1)$;

$\hat{M}(k)$ is the estimate of the moment from the measured velocity $\hat{\omega}(k)$ and the trajectory future velocity $\omega(k+1)$ to reach the trajectory point at time $(k+1)$.

For example, for BLDC motors, such defects can be considered as inter-turn faults, which lead to a decrease in resistance and inductance of the stator winding.

As originally proposed the Fault Detection and Isolation (FDI) filter is the first type of observer-based model generator. A full-order state observer can be realized as:

$$\hat{\mathbf{x}}_{k+1} = \mathbf{A}\hat{\mathbf{x}}_k + \mathbf{B}\mathbf{u}_{k+1} + \mathbf{L}(\mathbf{y}_k - \hat{\mathbf{y}}_k), \quad (6)$$

$$\hat{\mathbf{y}}_k = \mathbf{C}\hat{\mathbf{x}}_k + \mathbf{D}\mathbf{u}_k, \quad (7)$$

$$\mathbf{r}_k = \mathbf{y}_k - \hat{\mathbf{y}}_k. \quad (8)$$

where **L** is the observer matrix;
$\mathbf{r}_k$ is the magnitude of the residual.
In the case of normal operation of the motor, the value of residual is zero, the BLDC motor model transfer function $W_{yu}(z)$ can be realized as a defect detection filter.
In the case of normal operation of the motor, the following is true

$$\lim_{k\to\infty} \mathbf{r}_k = 0. \quad (9)$$

When a defect occurs, the residual $\mathbf{r}_k \neq 0$, which can be used as an indicator of a BLDC motor defect. However, in practice, disturbances are inevitable, so the residual $\mathbf{r}_k \neq 0$ cannot be unambiguously used to make any decision.

3 RESULTS AND DISCUSSION

The simulation results are obtained in SimInTech software package. Figure 1 shows a schematic of digital twin and defect BLDC motors with a digital twin with the following parameters: the coefficient of counter-EMF ke1=1.21, torque coefficient km1=0.95, moment of inertia J1=0.0031, armature winding resistance R1=14.6, armature winding inductance L1=0.248. The input voltage U=220 V and load resistance torque T=1.91 N·m in the form of a step. Figure 1 shows a digital twin and defective motors with inter-turn phase closure. The diagram compares the electric current of the defective BLDC motors with the electric current of the digital twin.

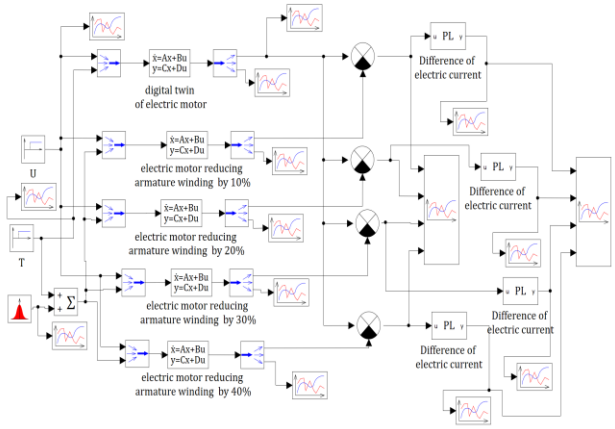

Figure 1. The schematic of digital twin and defect BLDC motors with resistance winding and its inductance decreased

As a result of interturn short-circuit, the resistance winding and its inductance decreased by 10%, 20%, 30%, 40%:
delta=0.9, R2=R1*delta, L2=L1*delta,
delta=0.8, R3=R1*delta, L3=L1*delta,
delta=0.7, R4=R1*delta, L4=L1*delta,
delta=0.6, R5=R1*delta, L5=L1*delta.

Figure 2 shows the graph of electric current residual of digital twin and defect BLDC motors model with resistance winding and its inductance decreased.
Four mean square deviations were calculated for each motor version, using the following formula:

$$\sigma = \frac{\sqrt{\sum_{i=0}^{N}(\omega_i - \omega_i^*)^2}}{i}, \quad (10)$$

where σ is mean square deviation, ωi and ωi* are angular velocities (ideal and real), N is number of measurements under acceleration.

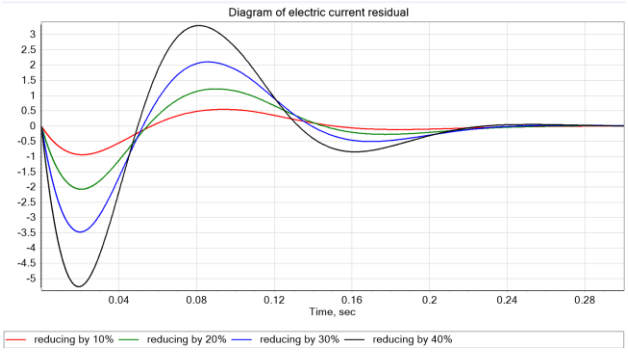

Figure 2. The diagram of electric current residual of digital twin and defect BLDC motors model with resistance winding and its inductance decreased

To calculate the mean square deviation, a program block was used where calculations were performed:
input u;
i=i+1;
summa1_kv = summa1_kv + u*u;
y = sqrt(summa1_kv/i);
output y;
Figure 3 shows a graph of the average square value of the electric current of digital twin and defect BLDC motors model with resistance winding and its inductance decreased.

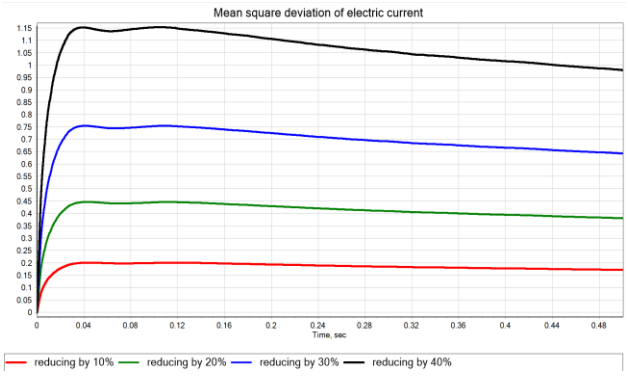

Figure 3. Graph of the average square value of the electric current of digital twin and defect BLDC motors model with resistance winding and its inductance decreased

Figure 4 shows a schematic of digital twin and defective motors with inter-turn phase closure. The diagram compares the angular velocity of defective BLDC motors with the angular velocity of the digital twin.

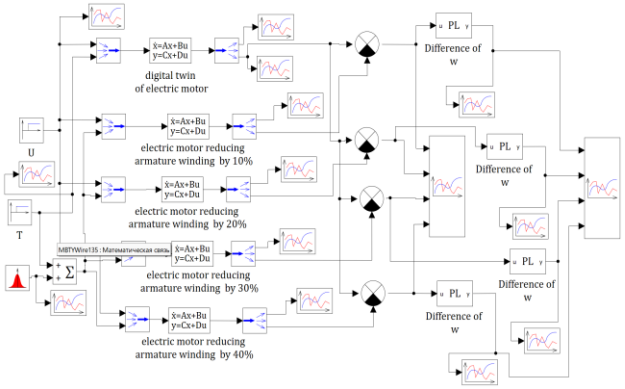

Figure 4. The schematic of digital twin and defect BLDC motors with resistance winding and its inductance decreased

Figure 5 shows the graph of angular velocity residual of digital twin and defect BLDC motors with resistance winding and its inductance decreased.
Figure 6 shows a graph of the average square value of the angular velocity of digital twin and defect BLDC motors with resistance winding and its inductance decreased.

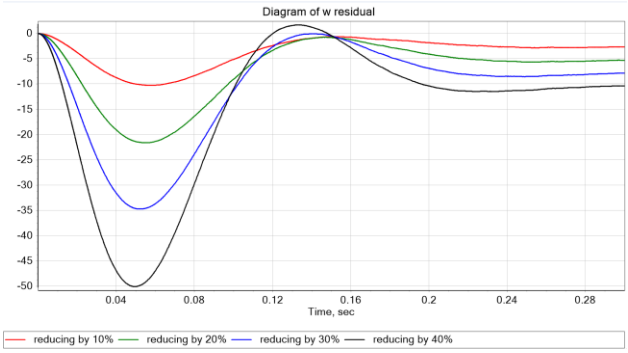

Figure 5. The graph of electric current residual of digital twin and defect BLDC motors with resistance winding and its inductance decreased

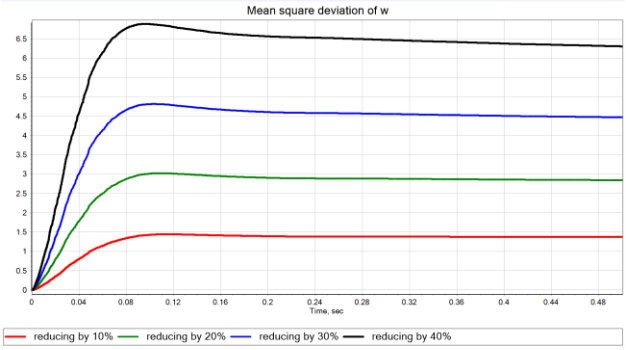

Figure 6. A graph of the average square value of the angular velocity of digital twin and defect BLDC motors model with resistance winding and its inductance decreased

The maximum values of the average square deviation in electric current and rotation speed of BLDC motors with resistance winding and its inductance decreased are shown in Table 1.

Table 1. The maximum values of the average square deviation in electric current and rotation speed

Defect BLDC motors with resistance winding and its inductance decreased	Maximum value of the mean square deviation of I	Maximum value of the mean square deviation of w
delta=0.9	0.20	1,49
delta=0.8	0.45	3.00
delta=0.7	0.75	4.80
delta=0.6	1.15	6.90

Figure 7 shows a schematic of digital twin and motors with resistance winding increased. The diagram compares the electric current of BLDC motors with resistance winding increased and digital twin.

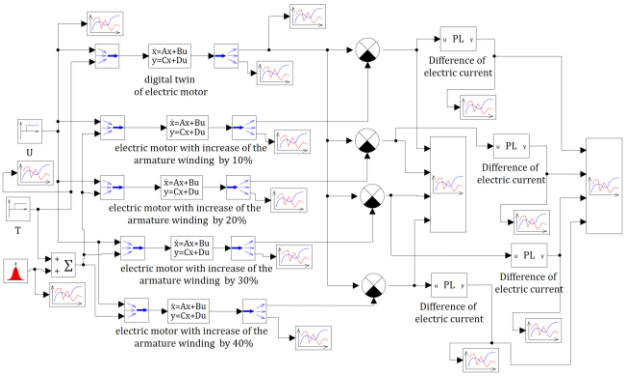

Figure 7. The schematic of digital twin and BLDC motors with resistance winding increased

Due to the heating of the motor, its winding resistance increases.
delta2=1.1, J2=J1, R2=R1*delta2, L2=L1,
delta3=1.2, J3=J1, R3=R1*delta3, L3=L1,
delta4=1.3, J4=J1, R4=R1*delta4, L4=L1,
delta5=1.4, J5=J1, R5=R1*delta5, L5=L1.

Figure 8 shows a graph of the average square value of the electric current of digital twin and BLDC motors with winding resistance increases.

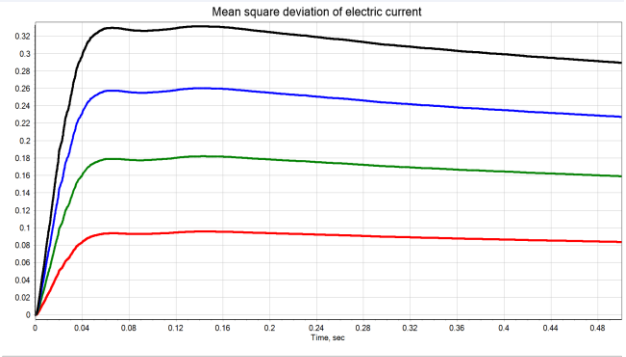

Figure 8. A graph of the average square value of the electric current of digital twin and BLDC motors model with resistance winding increased

Figure 9 shows a graph of the average square value of the angular velocity of digital twin and BLDC motors with winding resistance increases.

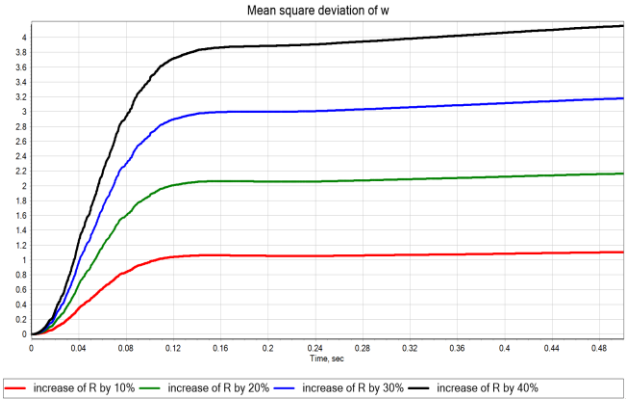

Figure 9. A graph of the average square value of the angular velocity of digital twin and BLDC motors model with resistance winding increased

The maximum values of the average square deviation in electric current and rotation speed of BLDC motors with resistance winding increased are shown in Table 2.

Table 2. The maximum values of the average square deviation in electric current and rotation speed of BLDC motors with resistance winding increased

Defect BLDC motors with resistance winding increased	Maximum value of the mean square deviation of I	Maximum value of the mean square deviation of w
delta=1.1	0.09	1,10
delta=1.2	0.18	1.95
delta=1.3	0.26	3.20
delta=1.4	0.33	4.19

The following computational experiments were carried out with an increase in the moment of inertia of the load:
delta2=1.1, J2=J1*delta2, R2=R1, L2=L1,
delta3=1.2, J3=J1*delta3, R3=R1, L3=L1,
delta4=1.3, J4=J1*delta4, R4=R1, L4=L1,
delta5=1.4, J5=J1*delta5, R5=R1, L5=L1.

Figure 10 shows a graph of digital twin and motors with an increase in the moment of inertia of the load. The diagram compares the electric current of BLDC motors with moment of inertia increased and digital twin.
Figure 11 shows a graph of the average square value of the electric current of digital twin and BLDC motors with an increase in the moment of inertia of the load.

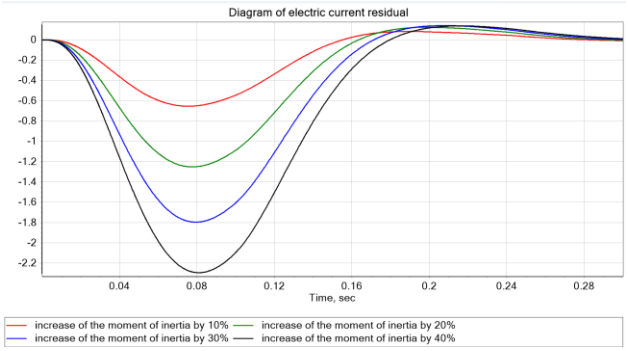

Figure 10. The graph of electric current residual of digital twin and defect BLDC motors with an increase in the moment of inertia of the load

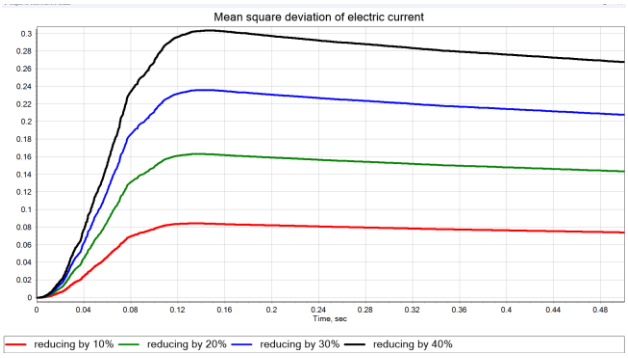

Figure 11. A graph of the average square value of the electric current of digital twin and defect BLDC motors model with an increase in the moment of inertia of the load

Figure 12 shows a graph of digital twin and motors with an increase in the moment of inertia of the load. The diagram compares the angular velocity of BLDC motors with moment of inertia increased and digital twin.

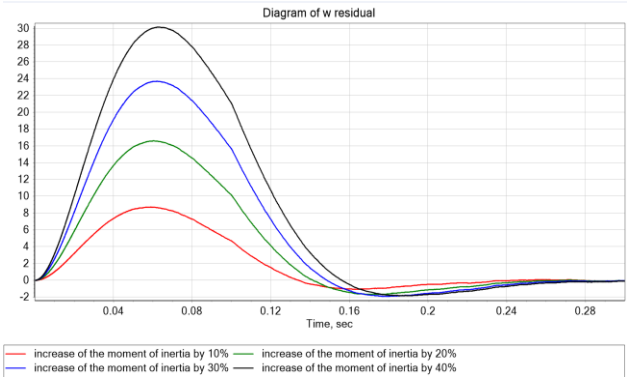

Figure 12. The graph of angular velocityresidual of digital twin and defect BLDC motors with an increase in the moment of inertia of the load

Figure 13 shows a graph of the average square value of the angular velocity of digital twin and BLDC motors with an increase in the moment of inertia of the load.

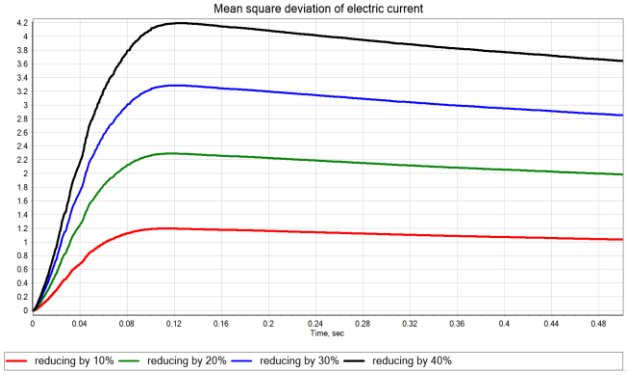

Figure 13. The graph of average square value of the angular velocity residual of digital twin and defect BLDC motors with an increase in the moment of inertia of the load

The maximum values of the average square deviation in electric current and rotation speed of BLDC motors with an increase in the moment of inertia of the load are shown in Table 3.

Table 3. The maximum values of the average square deviation in electric current and rotation speed an increase in the moment of inertia of the load of BLDC motors with resistance winding increased

Defect BLDC motors with resistance winding increased	Maximum value of the mean square deviation of I	Maximum value of the mean square deviation of w
delta=1.1	0.08	1,20
delta=1.2	0.16	2.30
delta=1.3	0.24	3.30
delta=1.4	0.30	4.20

4 CONCLUSIONS

A vector-matrix BLDC motors model in the state space has been developed, taking into account defects. It is proposed to use a discrepancy in electric current and angular velocity of rotation to diagnose BLDC motors. In case of motor defects, the resistance and inductance of the motor winding decrease compared to the reference model, which leads to an increase in the electric current discrepancy and the angular velocity of rotation of the BLDC motors. As the temperature increases during the operation of the BLDC motors, the discrepancy between the electric current and the angular velocity of the BLDC motors increases slightly. The BLDC motors are analyses using electric current and angular velocity sensors signals and the output signals of the digital twin. Based on the magnitude of the residual, the presence of defect in the BLDC motor is determined. If the defect value is insignificant, then appropriate maintenance actions are recommended. In case when the defect value is significant, it is necessary to perform emergency termination of the engine operation.

In further research it can be applied digital image processing, for example [Kurylo 2019, Karrach 2020, Frankovsky 2022]. The proposed model can be applied in automotive industry [Blatnicky 2020], or for specialized trolley [Ciertazsky 2025].

ACKNOWLEDGMENTS

The research was funded by the RSF grant No. 25-29-00792 and the study was carried out within grant from the RSF https://rscf.ru/en/project/25-29-00792/.

REFERENCES

[Blatnicky 2020] Blatnicky, M., Gerlici, J., Saga, et al. Design of a robotic manipulator for handling products of automotive industry. International Journal of Advanced Robotic Systems, 2020, Vol. 17, Issue 1. DOI: 10.1177/1729881420906290.

[Bozek 2021] Bozek, P., Nikitin, Yu., Krenicky, T. Diagnostics of Mechatronic Systems. Series: Studies in Systems, Decision and Control 345. Springer Nature, Switzerland AG, 2021, 79 p. DOI: 10.1007/978-3-030-67055-9.

[Chen 2021] Chen, H, Jiang, B, Ding, S.X. A broad learning aided data-driven framework of fast fault diagnosis for high-speed trains. IEEE Intelligent Transportation Systems Magazine, 2021, Vol. 13, No. 3, pp. 83-88. DOI: 10.1109/MITS.2019.2907629.

[Chen 2022] Chen, H., Liu, Z., Alippi, C., Huang, B., Liu, D. Explainable Intelligent Fault Diagnosis for Nonlinear Dynamic Systems: From Unsupervised to Supervised

Learning. IEEE Trans. on Neural Networks and Learning Systems, 2022. DOI: 10.1109/TNNLS.2022.3201511.

[Cheng 2022] Cheng, C., Wang, W., Ran, G., Chen, H. Data-Driven Designs of Fault Identification Via Collaborative Deep Learning for Traction Systems in High-Speed Trains. IEEE Trans Transp Electrif, 2022, Vol. 8, Iss. 2, pp. 1748-1757. DOI: 10.1109/TTE.2021.3129824.

[Cheng 2023] Cheng, C., Wang, Q., Nikitin, Y., et al. A data-driven distributed fault detection scheme based on subspace identification technique for dynamic systems. International Journal of Robust and Nonlinear Control, 2023, Vol. 33, Iss. 5, pp. 1-22. DOI: 10.1002/rnc.6554.

[Ciertazsky 2025] Ciertazsky, R., Vargovska, M., Pivarciova, E. Experimental Innovative Prototype Solution for a Specialized Handling Trolley for Sampling Devices. Machines, 2025, Vol. 13, Issue 9. DOI: 10.3390/machines13090775.

[Cioboata 2020] Cioboata, D., Neacsu, M. G., Stanciu, D., et al. Modelling and Simulation of a Brushless Motor DC for Electric Power Steering Assistance. Electrotehnica, Electronica, Automatica, 2020, Vol. 68, No. 3, pp. 22-31. DOI: 10.46904/eea.20.68.3.1108003.

[Demcak 2024] Demcak, J., Zidek, K., Krenicky, T. Digital Twin for Monitoring the Experimental Assembly Process Using RFID Technology. Processes, 2024, Vol. 12, 1512. DOI: 10.3390/pr12071512.

[Ding 2019] Ding, S.X. Application of randomized algorithms to assessment and design of observer-based fault detection systems. Automatica, 2019, Vol. 107, pp. 175-182. DOI: 10.1016/j.automatica.2019.05.037.

[Frankovsky 2022] Frankovsky, P., Delyova, I., Sivak, P., et al. Modal Analysis Using Digital Image Correlation Technique. Materials, 2022, Vol. 15, Issue 16. DOI: 10.3390/ma15165658.

[Halko 2014] Halko, J., Mascenik, J. Differential with an integrated, newly - developed two-stage transfer. Applied Mechanics and Materials, 2014, Vol. 510, pp. 215-219.

[Karrach 2020] Karrach, L., Pivarciova, E., Bozek, P. Identification of QR Code Perspective Distortion Based on Edge Directions and Edge Projections Analysis. Journal of Imaging, 2020, Vol. 6, Issue 7. DOI: 10.3390/jimaging6070067.

[Krenicky 2022] Krenicky, T., Nikitin, Y., Bozek, P. Model-Based Design of Induction Motor Control System in MATLAB. Applied Sciences, 2022, Vol. 12, 11957. DOI: 10.3390/ app122311957.

[Kurylo 2019] Kurylo, P., Pivarciova, E., Cyganiuk, J., Frankovsky, P. Machine Vision System Measuring the Trajectory of Upper Limb Motion Applying the Matlab Software. Measurement Science Review, 2019, Vol. 19, Issue 1. DOI: 10.2478/msr-2019-0001.

[Luo 2020] Luo, H., Yin, S., Liu, T., Khan, A.Q. A data-driven realization of the control-performance oriented process monitoring system. IEEE Trans. on Ind. Electronics, 2020, Vol. 67, pp. 521-530. DOI: 10.1109/TIE.2019.2892705.

[Mascenik 2022] Mascenik, J., Coranic, T. Experimental Determination of the Coefficient of Friction on a Screw Joint. Appl. Sci., 2022, Vol. 12, 11987. https://doi.org/10.3390/app122311987.

[Mohanraj 2022] Mohanraj, D., Aruldavid, R., Verma, R., et al. A Review of BLDC Motor: State of Art, Advanced Control Techniques, and Applications. IEEE Access, 2022, Vol. 10, pp. 54833-54869. DOI: 10.1109/access.2022.3175011.

[Nikitin 2020] Nikitin, Yu., Bozek P., Peterka, J. Logical-linguistic Model of Diagnostics of Electric Drivers with Sensors Support. Sensors, 2020, Vol. 20, Issue 16, pp. 1-19. DOI: 10.3390/s20164429.

[Nikitin 2022] Nikitin, Y., Krenicky, T., Bozek, P. Diagnostics of automated technological drives. Monitoring and Analysis of Manufacturing Processes in Automotive Production, Vol. 6. Lüdenscheid: RAM-Verlag, 2022, 148 p. ISBN 978-3-96595-018-4, e-ISSN 2629-3161.

[Patlolla 2021] Patlolla, S.V. Modelling of Brushless DC Motor Drive for Electric Vehicle Application. International Journal for Research in Applied Science and Engineering Technology, 2021, Vol. 9, pp. 2249-2258. DOI: 10.22214/ijraset.2021.35475.

[Xue 2018] Xue, T., Zhong, M., Ding, S.X., Ye, H. Stationary wavelet transform aided design of parity space vectors for fault detection in LDTV systems. IET Control Theory and Applications, 2018, Vol. 12, pp. 857-864. DOI: 10.1049/iet-cta.2017.1188.

[Yang 2015] Yang, Y., Ding, S.X., Li, L. On observer-based fault detection for nonlinear systems. Syst. Contr. Lett., 2015, Vol. 82, pp. 1399-1410. DOI: 10.1016/j.sysconle.2015.05.004.

[Zhang 2024] Zhang, Z., Xu, Q., Wang, Y. A New Sliding-Mode Observer-Based Deadbeat Predictive Current Control Method for Permanent Magnet Motor Drive. Machines, 2024, Vol. 12, No. 5, 297. DOI: 10.3390/machines12050297.

[Zhou 2018] Zhou, J., Yang, Y., Zhao, Z., Ding, S.X. A fault detection scheme for ship propulsion systems using randomized algorithm techniques. Control Engineering Practice, 2018, Vol. 81, pp. 65-72. DOI: 10.1016/j.conengprac.2018.09.008.

[Zhou 2020] Zhou, D., Zhao, Y., Wang, Z., He, X. and Gao, M. Review on diagnosis techniques for intermittent faults in dynamic systems. IEEE Trans. on Indus. Electronics, 2020, Vol. 67, No. 3, pp. 2337-2347. DOI: 10.1109/TIE.2019.2907500.

CONTACTS:

Nikitin Yury Rafailovich, Assoc. Prof. PhD.
Trefilov Sergei Aleksandrovich, Assoc. Prof. PhD.
Kalashnikov Izhevsk State Technical University
Mechatronic Systems Department
Studencheskaya 7, Izhevsk, 426069, Udmurtia
+79068164399, nikitin@istu.ru, trfefilov@istu.ru